complex. A similar explanation has been invoked to account for the failure of lactyl thiamin pyrophosphate to bind to wheat germ apopyruvate decarboxylase (Kluger & Smyth, 1981).

Neither imidazole (K_i = 0.003 M) (Rosenthaler et al., 1965) nor glycine methyl ester (K_i > 0.01 M) are good inhibitors of the decarboxylase although they are components of histidine methyl ester ($K_i = 8 \times 10^{-8}$ M). Effective inhibition is the result of incorporating these components into a single molecule. The binding advantage obtained from forming a single molecule is a factor of at least 3×10^3 (Jencks, 1975).

ACKNOWLEDGMENTS

We thank Louise Howell for assistance in preparing the manuscript.

Registry No. $AcCH_2CO_2Me$, 105-45-3; $AcCH_2CO_2H$, 541-50-4; histidine decarboxylase, 9024-61-7; L-histidine methyl ester, 1499-46-3; L-histidine ethyl ester, 7555-06-8; L-histidinamide, 7621-14-9; DL-3-amino-4-(4-imidazolyl)-2-butanone, 108212-43-7; acetoacetate decarboxylase, 9025-03-0.

REFERENCES

Battersby, A. R., Nicoletti, M., Staunton, J., & Vleggaar, R. (1980) *J. Chem. Soc., Perkin Trans. 1*, 43–51.

Chang, G. W., & Snell, E. E. (1968) *Biochemistry 7*, 2005–2012.

Crosby, J., Stone, R., & Lienhard, G. E. (1970) *J. Am. Chem. Soc. 92*, 2891–2900.

Gutowski, J. A., & Lienhard, G. E. (1976) *J. Biol. Chem. 251*, 2863–2866.

Huynh, Q. K., & Snell, E. E. (1986) *J. Biol. Chem. 261*, 4389–4394.

Jencks, W. P. (1975) *Adv. Enzymol. Relat. Areas Mol. Biol. 43*, 219–410.

Kluger, R., & Smyth, T. (1981) *J. Am. Chem. Soc. 103*, 1214–1216.

Lane, R. S., Manning, J. M., & Snell, E. E. (1976) *Biochemistry 15*, 4180–4185.

Mardashev, S. R., Simomina, L. A., Dabagov, N. S., & Gonchar, N. A. (1968) in *Pyridoxal Catalysis: Enzymes and Model Systems* (Snell, E. E., et al., Eds.) pp 451–467, Wiley Interscience, New York.

Mardashev, S. R., Gonchar, N. A., & Dabagov, N. S. (1969) *Dokl. Akad. Nauk SSSR 189*, 895–898.

Neuberger, A. (1944) *Biochem. J. 38*, 309–314.

Recsei, P. A., & Snell, E. E. (1970) *Biochemistry 9*, 1492–1497.

Swissman, E. E., & Weis, J. A. (1971) *J. Med. Chem. 14*, 945–947.

Stocker, F. B., Fordice, M. W., Larson, J. K., & Thorstenson, J. H. (1966) *J. Org. Chem. 31*, 2380–2383.

Vienozinskiene, J., Januseviciute, R., Pauliukonis, A., & Kazlauskas, D. (1985) *Anal. Biochem. 146*, 180–183.

Zerner, B., Coutts, S. M., Lederer, F., Waters, H. H., & Westheimer, F. H. (1966) *Biochemistry 5*, 813–816.

Construction and Evaluation of the Kinetic Scheme Associated with Dihydrofolate Reductase from *Escherichia coli*†

Carol A. Fierke,‡ Kenneth A. Johnson,§ and Stephen J. Benkovic*

Department of Chemistry, The Pennsylvania State University, University Park, Pennsylvania 16802

Received September 19, 1986; Revised Manuscript Received January 29, 1987

ABSTRACT: A kinetic scheme is presented for *Escherichia coli* dihydrofolate reductase that predicts steady-state kinetic parameters and full time course kinetics under a variety of substrate concentrations and pHs. This scheme was derived from measuring association and dissociation rate constants and pre-steady-state transients by using stopped-flow fluorescence and absorbance spectroscopy. The binding kinetics suggest that during steady-state turnover product dissociation follows a specific, preferred pathway in which tetrahydrofolate (H_4F) dissociation occurs after NADPH replaces $NADP^+$ in the ternary complex. This step, H_4F dissociation from the E·NADPH·H_4F ternary complex, is proposed to be the rate-limiting step for steady-state turnover at low pH because $k_{off} = V_M$. The rate constant for hydride transfer from NADPH to dihydrofolate (H_2F), measured by pre-steady-state transients, has a deuterium isotope effect of 3 and is rapid, k_{hyd} = 950 s^{-1}, essentially irreversible, K_{eq} = 1700, and pH dependent, pK_a = 6.5, reflecting ionization of a single group in the active site. This scheme accounts for the apparent pK_a = 8.4 observed in the steady state as due to a change in the rate-determining step from product release at low pH to hydride transfer above pH 8.4. This kinetic scheme is a necessary background to analyze the effects of single amino acid substitutions on individual rate constants.

Dihydrofolate reductase (DHFR)[1] (5,6,7,8-tetrahydrofolate:$NADP^+$ oxidoreductase) catalyzes the reduction of 7,8-dihydrofolate (H_2F) by NADPH to form 5,6,7,8-tetrahydrofolate (H_4F). Tetrahydrofolate is a coenzyme utilized in a number of one-carbon-transfer reactions and is essential for the biosynthesis of purines, thymidylate, and several amino acids. Hence, DHFR is a target for both anticancer and antibacterial drugs. DHFR has also been the subject of in-

† This work was supported in part by NIH Grants GM24129 and GM26726.

‡ Recipient of a National Institutes of Health postdoctoral fellowship (GM 10072).

§ Department of Biochemistry.

[1] Abbreviations: DHFR, dihydrofolate reductase; H_2F, dihydrofolate; H_4F, tetrahydrofolate; NADPH, nicotinamide adenine dinucleotide phosphate, reduced; $NADP^+$, nicotinamide adenine dinucleotide phosphate; TNADPH, thionicotinamide adenine dinucleotide phosphate, reduced; APADPH, acetylpyridine adenine dinucleotide phosphate, reduced; MTX, methotrexate; TMP, trimethoprim.

0006-2960/87/0426-4085$01.50/0

tensive structural and kinetic studies, including the study of mutant enzymes produced by site-directed mutagenesis (Villafranca et al., 1983; Chen et al., 1985; Howell et al., 1986; Taira et al., 1987a,b; Mayer et al., 1986). The structure of the *Escherichia coli*, *Lactobacillus casei*, and chicken liver enzymes have been determined to 1.7-Å resolution for some binary and ternary complexes (Bolin et al., 1982; Filman et al., 1982; Matthews et al., 1985). Binding kinetics of substrates and inhibitors to both *E. coli* (Cayley et al., 1981) and *L. casei* (Dunn & King, 1980; Dunn et al., 1978; Birdsall et al., 1980) DHFR have been studied, showing there is synergism in binding between the cofactor and folate binding sites. The steady-state mechanism has been studied with both initial velocity and progress-curve kinetics showing that the kinetic scheme conforms to random addition (Stone & Morrison, 1982), that steady-state turnover is pH dependent, owing to a single acidic active-site residue, and that the rate-limiting step at maximum turnover is not hydride transfer (Stone & Morrison, 1984; Howell et al., 1986; Chen et al., 1987).

Despite all this work there is still no coherent kinetic sequence that can explain the behavior of both wild-type and mutant enzymes. In the following study we describe the measurement of ligand binding and pre-steady-state transients by stopped-flow fluorescence with *E. coli* DHFR to isolate and measure individual rate constants in the DHFR mechanism. This collection of rate constants defines a complete kinetic scheme that can explain the DHFR steady-state behavior and that pinpoints the rate-determining step in turnover under a variety of conditions. This same set of experiments can also be used to study mutant enzymes and to determine the specific effects of the mutation.

Materials and Methods

Materials

Dihydrofolate (H_2F) was prepared from folic acid by the method of Blakley (1960), and (6*S*)-tetrahydrofolate (H_4F) was prepared from H_2F by using dihydrofolate reductase (Mathews & Huennekens, 1960) and purified on DE-52 resin eluting with a triethylammonium bicarbonate linear gradient (Curthoys et al., 1972). [4′(*R*)-^{2}H]NADPH, TNADPH (thionicotinamide adenine dinucleotide phosphate, reduced), and APADPH (acetylpyridine adenine dinucleotide phosphate, reduced) were prepared (Stone & Morrison, 1982) by using *Leuconostoc mesenteroides* alcohol dehydrogenase obtained from Research Plus, Inc., and purified by the method of Viola et al. (1979). Dihydrofolate reductase was purified from *E. coli* strain HB101 containing fol plasmid pTY1 (Taira et al., 1987a,b) by using a methotrexate affinity resin (Baccanari et al., 1977; Taira et al., 1987a,b). The concentration of tetrahydrofolate was determined spectrophotometrically by using a molar extinction coefficient of 28 000 M^{-1} cm^{-1} at 297 nm (Kallen & Jencks, 1966) or enzymatically by using a molar absorbancy change for the 10-formyl synthetase reaction of 12 000 M^{-1} cm^{-1} at 312 nm (Smith et al., 1981). The concentrations of NADPH, APADPH, and TNADPH were determined by using extinction coefficients of 6200 M^{-1} cm^{-1} at 339 nm, 9100 M^{-1} cm^{-1} at 363 nm, and 11 300 M^{-1} cm^{-1} at 395 nm, respectively (P-L Biochemicals, 1961). The concentration of H_2F was estimated spectrophotometrically by using a molar extinction coefficient of 28 000 M^{-1} cm^{-1} at 282 nm (Dawson et al., 1969). Concentrations of NADPH and H_2F were also determined enzymatically by using a molar absorbancy change for the dihydrofolate reductase reaction of 11 800 M^{-1} cm^{-1} at 340 nm (Stone & Morrison, 1982). The concentration of purified DHFR was determined spectrophotometrically at 280 nm by using a molar extinction coefficient of 31 100 M^{-1} cm^{-1} (D. Baccanari, personal communication) or by methotrexate titration (Williams et al., 1979). Interference filters used in the stopped-flow apparatus were obtained from Corion Corp.

Methods

Stopped-Flow Measurements. Kinetic data were obtained by using a stopped-flow apparatus built in the laboratory of Johnson (1986) that has a 1.6-ms dead time, a 2-mm path length, and a thermostated sample cell. Interference filters were used on both the input and output. Complex formation and pre-steady-state kinetics were obtained by using a 290-nm interference filter on the input and then monitoring either the quenching of the intrinsic enzyme fluorescence with an output filter at 340 nm or the enhancement of coenzyme fluorescence by energy transfer (Velick, 1958; Dunn & King, 1980) with an output filter at 450 nm. Coenzyme fluorescence was monitored by using a 340-nm input filter and 450-nm output filter. Transmittance measurements were made by using a 340-nm input filter and were later converted to absorbance. For slow reactions a neutral density filter (0.2–2.0 OD) was placed on the input to decrease the light intensity and thus decrease photobleaching of the sample. In most experiments the average of at least four runs was used for data analysis.

The data were collected over a given time interval by a computer. All data were analyzed by an iterative, nonlinear least-squares fit computer program using a modification of the method of moments (Dyson & Isenberg, 1971; Johnson, 1986). Kinetic data were analyzed with either a single-exponential, a single-exponential followed by a linear rate, or a double-exponential model. The data were then transferred to a Vax microcomputer, where a fit to more complicated models was tested by using the computer program SIMUL (Barshop et al., 1983).

Kinetic Measurements. Initial velocity for the reaction of DHFR with $NADP^+$ and H_4F was determined by measuring the rate of the enzyme-dependent increase at 340 nm by using a molar absorbancy difference of 11 800 M^{-1} cm^{-1} (Stone & Morrison, 1982), and the overall equilibrium constant was calculated from the total absorbance change. These studies were done in an anaerobic cuvette purged with argon, and the reaction was initiated by addition of DHFR.

The pre-steady-state and progress-curve kinetics were measured by using the stopped-flow apparatus. Dihydrofolate reductase (0.5–30 μM) was preincubated with NADPH (50–250 μM) to remove hysteretic behavior (Penner & Frieden, 1985) at various pH's, and the reaction was initiated by mixing with an equal volume of H_2F (2.5–200 μM) in the same buffer at 25 °C. The reaction was monitored by either absorbance, coenzyme fluorescence, or fluorescence energy transfer as described. A molar absorbancy change for this reaction of 8500 M^{-1} cm^{-1} by using a 340-nm band-pass filter was determined at low enzyme concentration as described (Stone & Morrison, 1982). A molar fluorescence change was established by this same method under the given experimental conditions.

The buffer contained 50 mM 2-(*N*-morpholino)ethanesulfonic acid, 25 mM tris(hydroxymethyl)aminomethane, 25 mM ethanolamine, and 100 mM sodium chloride (MTEN buffer). Over the pH range used, the ionic strength of this buffer remains constant (Ellis & Morrison, 1982). When H_4F was used as a substrate, the buffer was purged with argon and contained 1 mM dithioerythritol. The pH of the assay mixtures was determined at the temperature of the assay before and after the reaction.

Table I: Kinetic Binding Constants: Relaxation Method

ligand	enzyme species	pH 6.0 $k_{on} \times 10^7$ (M^{-1} s^{-1})	pH 6.0 k_{off} (s^{-1})	pH 9.0 $k_{on} \times 10^7$ (M^{-1} s^{-1})	pH 9.0 k_{off} (s^{-1})
NADPH	E	2.0 ± 0.1	3.5 ± 1.5	1.2 ± 0.1	2 ± 1
	E·H_4F	0.8 ± 0.03	85 ± 20		
	E·MTX	2.0 ± 0.2	<2	1.5 ± 0.3	<3
H_2F	E	4.2 ± 0.2	47 ± 10	4.0 ± 0.6	39 ± 9
	E·TNADPH[a]	2.5 ± 0.8	40 ± 10		
	E·$NADP^+$	2.6 ± 0.7	10 ± 5	5.6 ± 0.4	10 ± 5
$NADP^+$	E	1.3 ± 0.3	295 ± 25	1.2 ± 0.2	106 ± 14
	E·H_2F	0.5 ± 0.25	58 ± 12		
H_4F	E	2.4 ± 0.1	<1	2.7 ± 0.1	4 ± 2
	E·$NADP^+$	2.8 ± 0.3	5 ± 3		
	E·NADPH	0.23 ± 0.02	10 ± 3	0.2 ± 0.02	12 ± 2

[a] TNADPH is a very poor substrate for DHFR, $k_{cat} \leq 0.01$ s^{-1}.

Scheme I

$$L_1 + E_1 \underset{k_{off}}{\overset{k_{on}}{\rightleftharpoons}} E_1 \cdot L_1 + L_2 \underset{k_{off}'}{\overset{k_{on}'}{\rightleftharpoons}} E_1 \cdot L_1 \cdot L_2$$

$$k_{-2} \downarrow \uparrow k_2$$

$$E_2$$

Binding Constants. The association and dissociation rate constants were measured by stopped-flow fluorescence quenching (Dunn & King, 1980; Cayley et al., 1981) or energy transfer (Paulsen & Wintermeyer, 1986) at 25 °C in MTEN buffer as described. Equilibrium dissociation constants were also measured and analyzed as previously described (Birdsall et al., 1980; Stone & Morrison, 1982).

Results and Discussion

Binding Kinetics—Relaxation Methods. The rate of binding of ligands to DHFR in either the cofactor or the folate binding sites can be measured by following the quenching of intrinsic enzyme fluorescence. In the formation of binary complexes of DHFR at saturating substrate concentration, two exponentials of equal amplitude were observed: a rapid, ligand-dependent phase followed by a ligand-independent phase. In the formation of ternary complexes a single ligand-dependent exponential is observed as described by previous studies (Dunn et al., 1978; Dunn & King, 1980; Cayley et al., 1981). Cayley et al. (1981) concluded that this behavior is due to the mechanism shown in Scheme I, where substrate binds rapidly to only one of two enzyme conformers and interconversion between conformers is slow.

In the ligand-dependent reactions the observed first-order rate constants increased linearly with the substrate concentration, showing no sign of saturation. For a simple association reaction, the observed rate constant under pseudo-first-order conditions may be approximated by $k_{obsd} = k_{on}[L] + k_{off}$, where k_{on} and k_{off} are the association and dissociation rate constants, respectively. Thus, in a linear plot of k_{obsd} vs. [L] the slope is k_{on} and the intercept is k_{off}. Assuming a simple association reaction for the ligand-dependent phase, the association and dissociation rate constants for H_2F, H_4F, NADPH, and $NADP^+$ with both free enzyme and a variety of binary complexes were measured at pH 6 and 9, in MTEN buffer, 25 °C (see Table I). A representative plot of k_{obsd} vs. [L] is shown in Figure 1 for the ligand-dependent phase in binding H_4F to free DHFR.

Competition Experiments. The dissociation rate constant of a ligand from DHFR can also be measured by a competition experiment (Birdsall et al., 1980). In this technique the enzyme–ligand complex ($E \cdot L_1$) is mixed with a large excess of a second ligand that competes for the binding site (see Scheme II), and the formation of the new enzyme–ligand complex

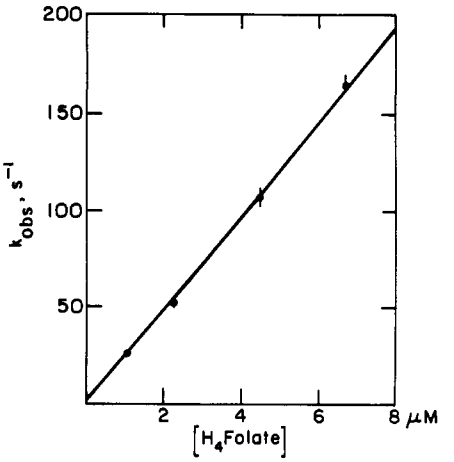

FIGURE 1: Concentration dependence of apparent rate constant for binding tetrahydrofolate (1–6 μM) to dihydrofolate reductase (0.25 μM) as measured by stopped-flow fluorescence quenching in MTEN buffer, pH 6.0, 25 °C.

($E \cdot L_2$) is monitored by a fluorescence change due to the difference in fluorescence quenching by the two ligands. When $k_1[L_1] \ll k_2[L_2] \gg k_{-1}$, k_{obsd} for this reaction is equal to the dissociation rate constant for L_1, k_{-1}. The validity of these conditions is checked by showing that k_{obsd} is independent of the concentration of L_2.

Scheme II

$$E \cdot L_1 \underset{k_1}{\overset{k_{-1}}{\rightleftharpoons}} E + L_1$$

$$E + L_2 \underset{k_{-2}}{\overset{k_2}{\rightleftharpoons}} E \cdot L_2$$

Figure 2 shows the measurement of the dissociation of H_4F from DHFR by mixing the enzyme–H_4F ($E \cdot H_4F$) complex with methotrexate (MTX) and observing a time-dependent decrease in the fluorescence signal. The rate constant for this reaction is independent of the concentration of MTX, DHFR, and H_4F. Dissociation rate constants determined with this technique for a variety of ligands in MTEN buffer, 25 °C, are shown in Table II. Identical product dissociation rate constants were measured from the product ternary complex, $E \cdot NADP^+ \cdot H_4F$, generated by two methods, either addition of products (H_4F and $NADP^+$) or addition of substrates (H_2F and NADPH) at low pH.

The results for the binding rate constants show that the assumption of a simple association step for the ligand-dependent step is reasonable. First, the dissociation rate constants measured by the two techniques, relaxation and competition, are identical within experimental error, showing that there are no slow isomerizations following association as has been ob-

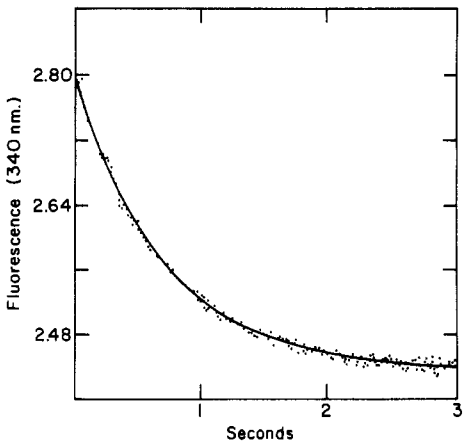

FIGURE 2: Measurement of dissociation rate constant, k_{off}, for tetrahydrofolate by diluting E·H_4F binary complex (4.4 μM H_4F, 1.0 μM DHFR) 2-fold into methotrexate (106.5 μM) and observing fluorescence quenching at 340 nm due to formation of E·MTX binary complex in MTEN buffer, pH 6.0, 25 °C. The data are fit by a single exponential decay.

Table II: Dissociation Rate Constants: Competition Method

ligand	enzyme species	trapping ligand	pH 6.0, k_{off} (s^{-1})	pH 9.0, k_{off} (s^{-1})
NADPH	E·NADPH	$NADP^+$	3.6 ± 0.5	3.3 ± 0.4
	E·H_4F·NADPH	$NADP^+$	85 ± 10	
$NADP^+$	E·$NADP^+$	NADPH	290 ± 20	109 ± 10
	E·H_4F·$NADP^+$	NADPH	200 ± 20	110 ± 10
	E·H_2F·$NADP^+$	TNADPH	50 ± 10	
H_2F	E·H_2F	MTX	22 ± 5	20 ± 2
	E·TNADPH·H_2F	MTX	43 ± 6	
	E·$NADP^+$·H_2F	MTX	6.6 ± 1	4.6 ± 1
H_4F	E·H_4F	MTX	1.4 ± 0.2	2.4 ± 0.3
	E·$NADP^+$·H_4F	MTX	2.4 ± 0.2	5.7 ± 0.7
	E·NADPH·H_4F	MTX, TMP	12 ± 2	18 ± 2

Table III: Comparison of Equilibrium and Kinetic Binding Constants at pH 6 and 25 °C in MTEN Buffer

	k_{off}/k_{on} (μM)	K_D (μM)
NADPH	0.18 ± 0.04	0.33 ± 0.06[a]
$NADP^+$	22 ± 7	24 ± 4[b]
H_4F	0.06 ± 0.01	0.1 ± 0.01[b]
H_2F	0.5 ± 0.3	0.22 ± 0.06[a]

[a] K. Taira and S. J. Benkovic, personal communication. [b] This paper.

served with the inhibitor methotrexate (Williams et al., 1979; Blakley & Cocco, 1985b). Second, the relationship between the ratio k_{off}/k_{on} and the dissociation constant K_D depends on the equilibrium between two enzyme conformations (Scheme I), where $K_{eq} \simeq 1$ in agreement with the observations of Cayley et al. (1981). Consequently, the measured K_D should be 2-fold larger than the ratio of k_{off}/k_{on} (eq 1). This is true

$$K_D = (k_{off}/k_{on})[(K_{eq} + 1)/K_{eq}] \quad (1)$$

for the binding of NADPH and H_4F, whereas the K_D's for H_2F and $NADP^+$ are smaller than predicted (Table III) from the rate measurements.

The binding experiments suggest likely rate-determining steps for both V_M and V/K during steady-state turnover at low pH. The measured V/K value (varying H_2F), 2 × 10^7 M^{-1} s^{-1} (Stone & Morrison, 1984), is similar to the association rate constant for H_2F to E·TNADPH (thionicotinamide adenine dinucleotide phosphate, reduced), suggesting that this is the rate-determining step for V/K. The dissociation rate constant for H_4F from either E or E·$NADP^+$ is 1.4 s^{-1} or 2.4 s^{-1}, respectively, both of which are slower than the observed V_M of 12 s^{-1}. Thus these steps cannot be part of the predominant pathway during steady-state turnover. However, the H_4F dissociation rate is increased to 12 s^{-1} by binding NADPH to E·H_4F, which then must be the primary rate-limiting step under V_M conditions. The dissociation rates thus favor a specific, preferred pathway of product dissociation which is in accord with the negative synergism between folinic acid and coenzyme binding to *L. casei* DHFR observed by Birdsall et al. (1981). This pathway avoids the formation of any free E during the steady state and hence the possibility of forming any inactive enzyme conformer.

The binding experiments also indicate that H_2F and $NADP^+$ show positive synergistic binding upon forming the abortive ternary complex E·H_2F·$NADP^+$. The ratios of k_{off}/k_{on} for H_2F and $NADP^+$ dissociation are 0.2 and 10 μM, respectively. Thus, H_2F binds to E·$NADP^+$ 5-fold better than to E·NADPH; $NADP^+$ binds to E·H_2F about 4-fold better than to E·H_4F (reference values are taken from Scheme IV). This suggests that the E·H_2F·$NADP^+$ complex will build up during steady-state turnover when both $NADP^+$ and H_2F are present. This is consistent with the findings of Morrison and Stone (1982) and M. H. Penner and C. Frieden (personal communication).

The magnitude of the association rate constants for H_2F and NADPH are faster than those measured by Cayley et al. (1981), while the dissociation rate constants and other kinetic parameters are similar. The discrepancy is due to the variation in salt concentrations, 0.1 vs. 0.5 M sodium chloride, and implies that the association rates are ionic strength dependent, particularly for NADPH binding. The association and dissociation rate constants for binding to *E. coli* DHFR, as well as the equilibrium K_D's, show little or no pH dependence (Stone & Morrison, 1983; K. Taira and S. J. Benkovic, personal communication), contrary to the results obtained with *Streptococcus faecium* DHFR (Blakley & Cocco, 1985a).

Pre-Steady-State Experiments. The above experiments implicate H_4F dissociation as the rate-limiting step during steady-state turnover at low pH and require there be a burst of product formation during the first turnover. This hypothesis was tested by mixing the enzyme–NADPH binary complex with H_2F and measuring the rate of product formation by either UV absorbance, fluorescence, or fluorescence energy transfer stopped-flow spectroscopy as described under Methods. In all three cases a pre-steady-state burst of product formation was observed. The fluorescence energy transfer experiments provided the largest pre-steady-state to steady-state signal ratio, so this technique was used in further studies. The set of interference filters used for these experiments allows observation of a small amount of substrate fluorescence. Thus, the observed steady-state rate is due to a decrease in the substrate concentration that is being observed along with enzyme–ligand complexes. Figure 3 shows an example of the pre-steady-state burst observed by stopped-flow fluorescence energy transfer, pH 6.5, 25 °C. These data are fit well by a single exponential, k^H = 450 s^{-1}, followed by a linear rate, V_M = 12 s^{-1}. On the basis of absorbance measurement, this transient represents the formation of 0.9 ± 0.1 mol of product/mol of enzyme. The pre-steady-state rate is independent of H_2F concentration at high levels (40–160 μM) but becomes linearly dependent at low levels (<10 μM) when H_2F binding to E·NADPH becomes rate determining, k_{obsd} = (5 ± 1) × 10^7 M^{-1} s^{-1}. A similar result was obtained when the enzyme was preincubated with H_2F and the reaction was initiated by addition of NADPH. At low concentrations of NADPH (≤20 μM) the rate constant is linearly dependent on the NADPH concentration, k_{obsd} = (5.2 ± 0.7) × 10^6 M^{-1} s^{-1}, while at larger

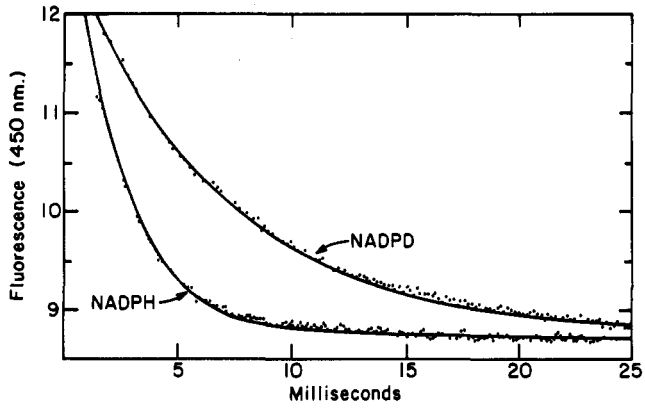

FIGURE 3: Measurement of the pre-steady-state burst by stopped-flow fluorescence energy transfer. DHFR is preincubated with either NADPH or [4′(*R*)-^{2}H]NADPD, and the reaction is initiated by addition of H_2F. Final conditions are 15 μM DHFR, 125 μM NADPH(D), 100 μM H_2F, MTEN buffer, pH 6.5, 25 °C. The data are fit by a single exponential decay followed by a linear, steady-state rate, V_M = 12 s^{-1}.

concentrations the rate constant levels off at $\simeq$450 s^{-1}.

Figure 3 also shows that the pre-steady-state burst measured with stereospecifically labeled [4′(*R*)-^{2}H]NADPD is fit by a slower single exponential, k^D = 150 s^{-1}, followed by the same linear rate. Identical rate constants are obtained from either a nonlinear least-squares fit or computer simulations by using SIMUL with the other rate constants shown in Schemes IV and V. The pre-steady-state rate constant has a deuterium isotope effect, k^H/k^D = 3, at pH 6.5. A similar isotope effect was measured at pH 5.0 and 8.0. Thus, at high concentrations of H_2F, hydride transfer is at least partially, and perhaps completely, rate-limiting in the pre-steady state. Two pieces of evidence suggest that an isotope effect of 3 may be the maximum observed for this reaction in the absence of other nonobservable steps. A similar isotope effect is observed (1) during steady-state turnover by DHFR at high pH where hydride transfer is rate-limiting, k^H/k^D = 3 (Chen et al., 1987), and (2) in an enzymic model reduction of an imine by NADH, k^H/k^D = 3.8 (Srinivasan & Fisher, 1985).

The pre-steady-state burst shows a marked pH dependence with both the rate constant and the amplitude of the burst decreasing as the pH increases, although with different pK_a's as shown in Figure 4. The pH dependence of the observed rate constant is well described by a single pH-dependent step with pK_a = 6.5 ± 0.1 and k_{max} = 950 ± 50 s^{-1}, followed by a pH-independent step with a rate constant of 12 s^{-1}. It is likely that the pK_a observed in the pre-steady-state rate represents the true pK_a for the enzyme ternary complex, E·H_2F·NADPH, and that k_{max} is the rate of hydride transfer from the fully protonated species since the observed isotope effect is constant throughout the pH range. Moreover the proton-transfer component of the chemical step is fast because (1) the observed pre-steady-state transient is a single exponential at all pH values in accord with rapid equilibrating E·H_2F·NH ⇌ H·E·H_2F·NH (a slow proton-transfer step would show a biphasic decay of fluorescence) and (2) the pH dependence appears in the observed pre-steady-state rate and not in the associated amplitude (pH 5–7.5). At higher pH the decrease in amplitude results from the change in the rate-limiting step in V_M from H_4F release to hydride transfer.

In these experiments, the fluorescence signal measured at 450 nm is due to excitation of the dihydronicotinamide fluorescence of the coenzyme via energy transfer from the enzyme. Energy transfer has a $1/R^6$ distance dependence (Lakowicz, 1983) and is significant only when NADPH is bound to the enzyme. The pre-steady-state fluorescence energy transfer signal monitors the net transformation of E·NADPH·H_2F → E·NADPH·H_4F (the species that accumulates in the steady state). Evidence that this reaction occurs in two steps, first hydride transfer to form E·NADP$^+$·H_4F, which is accompanied by a large signal decrease, followed by ligand exchange to form E·NADPH·H_4F, which is accompanied by little or no signal change, has been drawn from several observations. (1) When NADPH and DHFR were mixed, a time-dependent increase in the fluorescence energy transfer was observed with the same constant as for NADPH binding measured by fluorescence quenching. This signal was not altered by trimethoprim and presumably by H_2F binding. (2) When E·NADPH was mixed with high concentrations of NADP$^+$ the fluorescence energy transfer signal decreases with a rate constant equal to k_{off} for NADPH. (3) Formation of the abortive E·NADPH·H_4F complex from E·NADPH occurred with a time-dependent decrease in fluorescence energy

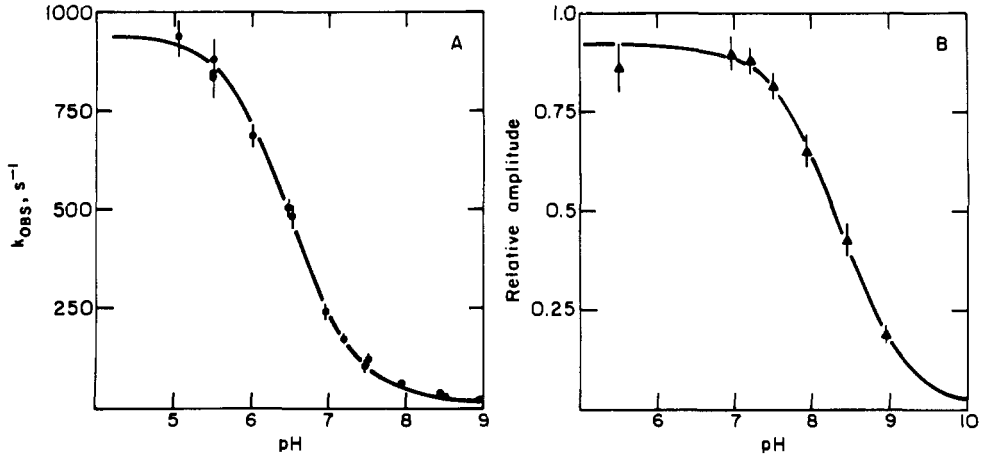

FIGURE 4: (A) Rate constant for the pre-steady-state burst measured by stopped-flow fluorescence energy transfer as a function of pH. Final conditions are 10 μM DHFR, 100 μM H_2F, and 125 μM NADPH in MTEN buffer, 25 °C. The solid line is theoretical, assuming k_{hyd} = 950 s^{-1}, pK_a = 6.5, and V_M = 12 s^{-1}. (B) Relative amplitude for the pre-steady-state burst measured by stopped-flow fluorescence energy transfer as a function of pH. Final conditions are as in (A). The solid line is theoretical (Johnson, 1983), assuming the process

$$\text{E·H}_2\text{F·NH} \xrightarrow{k_{obsd}} \text{E·H}_4\text{F·N} \xrightarrow{k_3} \text{E·H}_4\text{F} \xrightarrow{\text{fast}} \text{E·H}_4\text{F·NH} \xrightarrow{k_7} \text{E·NH} + \text{H}_4\text{F}$$

where $k_{obsd} = 950/(1 + K_a/[H^+])$, k_3 = 200 s^{-1}, and k_7 = 12 s^{-1}. The equations used to fit these data are approximations. The exact solution for each pH was modeled by using SIMUL, which gave the same conclusions.

transfer with the same rate constant as that for H_4F binding as measured by fluorescence quenching. Also, production of E·NADPH·H_4F from E·$NADP^+$·H_4F results in no observable fluorescence energy transfer change. Thus, any ternary complexes ($NADP^+$/NADPH) with H_4F present exhibit no appreciable energy transfer. Two additional tangential experiments support this hypothesis: (i) replacement of H_4F in E·NADPH·H_4F by MTX restores the energy transfer process and (ii) incubation of E·NADPH with various concentrations of H_4F prior to initiating turnover by mixing with H_2F does not affect the observed rate constant for hydride transfer but decreases its amplitude with an apparent half-maximal inhibition of 4 ± 1 μM H_4F, similar to the measured ratio of k_{off}/k_{on} = 5 ± 1 μM (Tables I and II) for H_4F binding to E·NADPH.

Reverse Reaction and Overall Equilibrium Constant. The equilibrium constant for the formation of $NADP^+$ and H_4F from NADPH and H_2F was measured by adding DHFR (0.3 μM) to a mixture of H_4F and $NADP^+$ and measuring the total increase in absorbance at 340 nm, which allows calculation of the equilibrium concentration of NADPH and H_2F by using the extinction coefficient for the overall reaction. This equilibrium constant was measured in MTEN buffer, 25 °C, under a variety of $NADP^+$ concentrations (0.9–3.6 mM), H_4F concentrations (44–178 μM), and pH's (8.0–9.8) to be K_{ov} = (1.3 ± 0.3) × 10^{11} M^{-1} for the reaction shown in Scheme III, which is consistent with previously measured values of 8.4 × 10^{10} M^{-1} (Nixon & Blakley, 1968) and 1.6 × 10^{11} M^{-1} (Mathews & Huennekens, 1965).

Scheme III

$$\text{NADPH} + H_2F + H^+ \xrightleftharpoons{K_{ov},\ \text{DHFR}} H_4F + NADP^+$$

$$E + H \underset{K_a}{\rightleftharpoons} {}^{H}E + \text{NADPH} + H_2F \underset{K_2}{\rightleftharpoons}$$

$${}^{H}E^{\text{NADPH}}_{H_2F} \underset{K_{eq}}{\rightleftharpoons} E^{NADP^+}_{H_4F} \underset{K_4}{\rightleftharpoons} E + NADP^+ + H_4F$$

The rate of the reverse reaction (net conversion of H_4F and $NADP^+$ to form H_2F and NADPH) was measured in the steady state from the increase in absorbance at 340 nm. The rate was 0.041 ΔOD_{340}/min, when DHFR (0.128 μM) was added to H_4F (178 μM) and $NADP^+$ (1.97 mM) in MTEN buffer, pH 8.9, 25 °C. The rate of this reaction was virtually unaffected when the concentration of either substrate was halved, which implies that these are saturating conditions, so V_M = 0.48 ± 0.03 s^{-1}. The pH dependence of this reaction (pH 7–10, data not shown) can be fit with a single pK_a of 7.8 ± 0.2 and a maximal rate constant at high pH, V_M = 0.55 ± 0.1 s^{-1}. This rate constant reflects the rate of hydride transfer from H_4F to $NADP^+$ on the enzyme since this step is rate determining in the forward direction at high pH (k^H/k^D = 3.0; Chen et al., 1987) and the measured product (H_2F and NADPH) dissociation rate constants are fast.

The internal equilibrium constant for the formation of H_4F and $NADP^+$ can now be calculated, K_{eq} = 950 s^{-1}/0.6 s^{-1} = (1.6 ± 0.3) × 10^3, and is much smaller than K_{ov}. This equilibrium constant can be scaled to the overall equilibrium within experimental error (Scheme IV), where $K_{ov} = (K_{eq})(1/K_a)(K_4/K_2) = (1.6 \times 10^3)(10^{6.5})(13) = (6.5 \pm 4) \times 10^{10}$. Our calculation suggests that the major factor in decreasing the equilibrium constant on the enzyme is the decreased acidity of the enzyme acid, pK_a = 6.5, compared to that of hydronium ion, pK_a = 0.

Summary of Overall Kinetic Scheme. Measurements of the various association and dissociation rate constants and of the forward and reverse rate constants for hydride transfer have been described. From these an overall kinetic sequence at low pH has been formulated (Scheme IV); its pH dependence is shown in Scheme V. The association and dissociation rate constants of the binary complexes and all of the ternary complexes except E·H_2F·NADPH have been measured directly. The association rate constants for binding H_2F to E·NADPH or NADPH to E·H_2F to form the reactive ternary complex, E·H_2F·NADPH, were measured in single turnover experiments under conditions where formation of the ternary complex was slower than hydride transfer. The dissociation rate constants of H_2F and NADPH from this complex were more difficult to estimate by using the techniques in this paper. For H_2F dissociation, TNADPH was chosen as the best NADPH analogue so $k_{off} \simeq 40$ s^{-1}. There is no good way to estimate k_{off} for NADPH from this complex since there is evidence that NADPH binding in ternary complexes with either MTX or H_4F is very different than in a ternary complex with H_2F. Thus the value for k_{off} for NADPH from E·NADPH·H_2F was chosen to balance the equilibrium binding within the closed system. The heavy arrows in Scheme IV indicate the kinetic pathway for steady-state turnover at saturating substrate conditions. This scheme omits the addition of a proton to the enzyme in the transformation of E·$NADP^+$·H_4F to E·NADPH·H_2F via ligand exchange since it is not known at which step this occurs.

The pH dependence of this reaction is illustrated in Scheme V. A single pK_a of 6.5 is observed in the pre-steady state that is the pK_a for the E·NADPH·H_2F ternary complex. The pK_a's

Scheme IV: pH-Independent Kinetic Scheme for Dihydrofolate Reductase at 25 °C in MTEN Buffer[a]

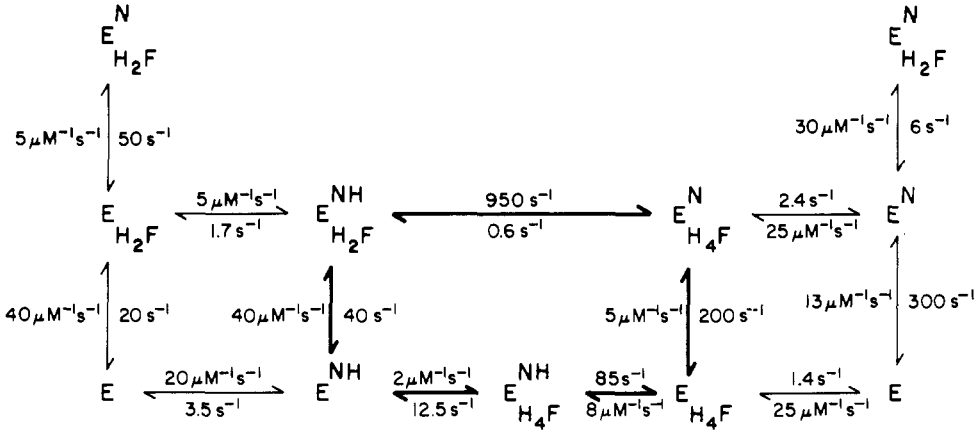

[a] N, $NADP^+$; NH, NADPH; H_2F, dihydrofolate; H_4F, tetrahydrofolate.

Scheme V: pH-Dependent Kinetic Scheme for Dihydrofolate Reductase at 25 °C in MTEN Buffer[a]

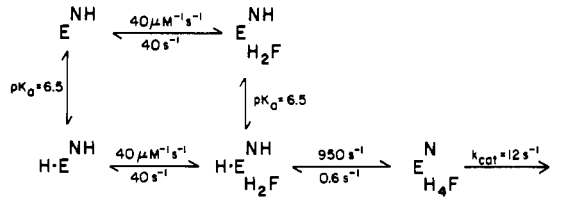

[a] N, $NADP^+$; NH, NADPH; H_2F, dihydrofolate; H_4F, tetrahydrofolate.

Table IV: Predicted Steady-State Parameters in MTEN Buffer at 25 °C

	predicted	measured
100 μM NADPH, varying H_2F		
V_M	11.5	12.3 ± 0.7[a]
pK_a	8.4	8.4[b]
k^H/k^D (pH 10.0)	2.8	2.9 ± 0.08[c]
k^H/k^D (pH 8.0)	1.52	1.78 ± 0.07[c]
k^H/k^D (pH 6.0)	1.02	1.0 ± 0.1[c]
V/K	3.6×10^7	$(1.8 \pm 0.3) \times 10^7$[a]
pK_a	7.90	8.1[b]
k^H/k^D (pH 10.0)	2.8	3.19 ± 0.22[c]
k^H/k^D (pH 8.0)	2.00	1.91 ± 0.25[c]
K_M (H_2F) (μM)	0.32	0.7 ± 0.2[a]
10 μM H_2F, 1–100 μM NADPH, pH 7.0		
V_M	10.5 s^{-1}	10 ± 1[a]
V/K	2.1×10^6	$(2.1 \pm 0.7) \times 10^6$[a]
K_M (NADPH) (μM)	5.0	4.8 ± 1[a]
180 μM H_4F, 2 mM $NADP^+$		
V_M	0.50 s^{-1}	0.55 ± 0.1[a]
pK_a	7.8	7.8 ± 0.2[a]

[a] Steady-state parameters measured in MTEN buffer, 25 °C, as described in this paper and by Stone and Morrison (1982). [b] Data taken from Stone and Morrison (1984). [c] Data taken from Chen et al. (1987).

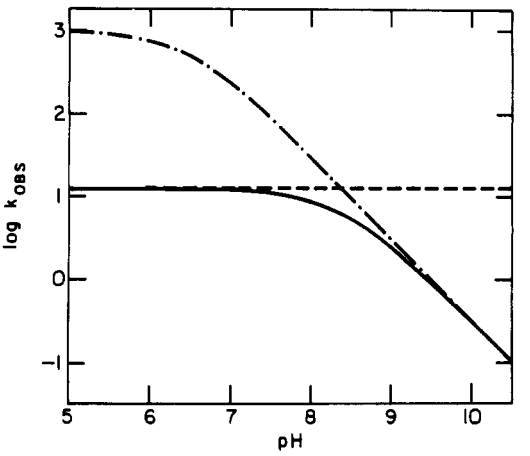

FIGURE 5: Observed rate constants for hydride transfer (–·–), H_4F dissociation (– – –), and V_M (—) as a function of pH.

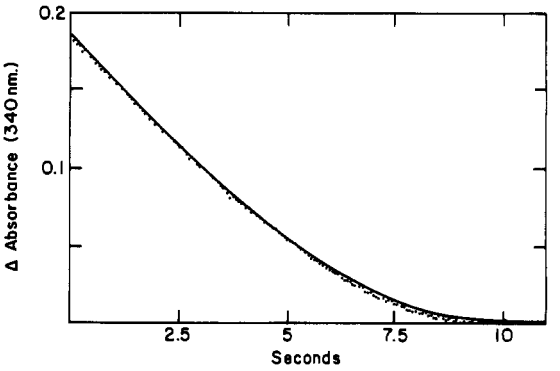

FIGURE 6: Full time course curve as measured by stopped-flow absorbance. DHFR is preincubated with NADPH, and the reaction is initiated by addition of H_2F. Final conditions are 1.6 μM DHFR, 110 μM H_2F, and 140 μM NADPH in MTEN buffer, pH 6.5, 25 °C. The curve was simulated by the computer program SIMUL using Schemes IV and V.

for free enzyme and enzyme–substrate binary complexes (E·H_2F and E·NADPH) are also estimated to be 6.5 since there is little or no pH dependence on substrate binding. It is possible that the observed pK_a is higher than the true pK_a if the observed rate plateaus owing to a new rate-limiting step that is slower than hydride transfer from the fully protonated ternary complex. This is unlikely since the observed isotope effect on the pre steady state remains constant at low pH. In this study there is no evidence for slow (<1000 s^{-1}) proton transfer between either enzyme and solvent or enzyme and H_2F. As discussed below, a pK_a of 6.5 for the ternary complex can account for the single pK_a of 8.4 measured for steady-state turnover (Stone & Morrison, 1984). The pK_a of 6.5 for the E·NADPH·H_2F ternary complex is due to the ionization of Asp-27 at the active site of DHFR as has been proposed for the steady-state pK_a (Howell et al., 1986). This pK_a is similar to the pK_a of 6.3 for an unbound enzyme suggested by Stone and Morrison (1983) from the pH dependence of 2,4-diamino-6,7-dimethylpteridine binding.

Predictions. A good test of the validity of Schemes IV and V is a comparison of the measured steady-state parameters with those predicted by this model as shown in Table IV. Steady-state kinetic parameters for the proposed model (Schemes IV and V) were determined by double-reciprocal plots of data simulated by using the computer program SIMUL (Barshop et al., 1973) at a variety of substrate concentrations and pHs. This model assumed that the binding rate constants have no pH dependence, which is only an approximation. The isotope effect data were simulated by using an isotope effect on hydride transfer of 3. As can be seen in Table IV, the predictions are quite close to the observed data under all the conditions. When NADPH is varied, a biphasic dependence on NADPH concentration might be expected since NADPH binding occurs at two points in this model. In both the simulated and observed data at pH 7, 1–100 μM NADPH, the double-reciprocal plots are virtually linear, suggesting that the second K_M is too small to be observed.

Figure 5 shows the pH dependence for the hydride transfer and H_4F dissociation rate constants. This figure illustrates the change in the steady-state rate-limiting step from H_4F dissociation at low pH to hydride transfer at high pH and consequently the change in the pK_a controlling the pre-steady-state and steady-state rates from pK_a 6.5 to 8.4. The change in the magnitude of the observed steady-state deuterium kinetic isotope effect parallels the change in the steady-state rate-limiting step. The displacement of the pH dependency for V/K results from the nonequilibrium binding of H_2F. The observed pK_a is estimated from the relationship pK_a(obsd) = 6.5 + log (950/40) (Cleland, 1977, 1982), where 40 s^{-1} is the dissociation rate for H_2F from E·H_2F·NH. This pK_a(obsd) also controls the pH dependency of V_M in the reverse direction.

A second test of the validity of the proposed model is to determine whether it will predict the full time course kinetics (Stone & Morrison, 1982; M. H. Penner and C. Frieden, personal communication) of DHFR. Figure 6 shows the full time course for the reaction of DHFR with NADPH (140 μM) and H_2F (110 μM), pH 6.5, 25 °C, as measured by stopped-

flow absorbance. The solid line in this figure is data simulated by the computer program SIMUL using Schemes IV and V under the given experimental conditions. This model will also predict the full time course kinetics at low concentrations of substrates (≤ 20 μM, data not shown) and consequently accounts for all the observed steady-state behavior.

Previous studies based on steady-state kinetics (Stone & Morrison, 1984) suggested that the rate-determining step occurs before hydride transfer. The burst of product formation observed in the first turnover shows that this cannot be true; the rate-determining step must occur after hydride transfer. M. H. Penner and C. Frieden (personal communication) have recently proposed a similar model. Studies on two mutant DHFR enzymes, Phe-31 → Tyr and Phe-31 → Val (Chen et al., 1987), show that these mutations increase the k_{off} for H_4F, which is translated into a parallel increase in the observed steady-state turnover rate, as predicted by the wild-type kinetic scheme. Thus, the model shown in Schemes IV and V can account for the observed kinetic behavior of the wild-type DHFR and can now be used to understand the effect of a single amino acid substitution on individual rate constants.

ACKNOWLEDGMENTS

We thank our colleagues, Jin-Tan Chen, Kazunari Taira, and Lawrence F. Courtney, for their many helpful suggestions.

REFERENCES

Baccanari, D. P. Averett, D. Briggs, C., & Burchall, J. (1977) *Biochemistry 16*, 3566–3572.

Barshop, B. A., Wrenn, R. F., & Frieden, C. (1983) *Anal. Biochem. 130*, 134–145.

Birdsall, B., Burgen, A. S. V., & Roberts, G. C. K. (1980) *Biochemistry 19*, 3723–3731.

Birdsall, B., Burgen, A. S. V., Hyde, E. I., Roberts, G. C. K., & Feeney, J. (1981) *Biochemistry 20*, 7186–7195.

Blakley, R. L. (1960) *Nature (London) 188*, 231–232.

Blakley, R. L., & Cocco, L. (1985a) *Biochemistry 24*, 4704–4709.

Blakley, R. L., & Cocco, L. (1985b) *Biochemistry 24*, 4772–4777.

Bolin, J. T., Filman, D. J., Matthews, D. A., Hamlin, R. C., & Kraut, J. (1982) *J. Biol. Chem. 257*, 13650–13662.

Cayley, P. J., Dunn, S. M. J., & King, R. W. (1981) *Biochemistry 20*, 874–879.

Chen, J.-T., Mayer, R. J., Fierke, C. A., & Benkovic, S. J. (1985) *J. Cell. Biochem. 29*, 73–82.

Chen, J.-T., Taira, K., Tu, C.-P. D., & Benkovic, S. J. (1987) *Biochemistry* (following paper in this issue).

Cleland, W. W. (1977) *Adv. Enzymol. Relat. Areas Mol. Biol. 45*, 273–387.

Cleland, W. W. (1982) *Methods Enzymol. 87*, 390–404.

Curthoys, H. P., Scott, J. M., & Rabinowitz, J. C. (1972) *J. Biol. Chem. 247*, 1959–1964.

Dawson, R. M. C., Elliott, D. C., Elliott, W. H., & Jones, K. M. (1969) *Data for Biochemical Research*, Oxford University Press, Oxford.

Dunn, S. M. J., & King, R. W. (1980) *Biochemistry 19*, 766–773.

Dunn, S. M. J. Batchelor, J. G., & King, R. W. (1978) *Biochemistry 17*, 2356–2364.

Dyson, R. D., & Isenberg, I. (1971) *Biochemistry 10*, 3233–3241.

Ellis, K. J., & Morrison, J. F. (1982) *Methods Enzymol. 87*, 405–426.

Filman, D. J., Bolin, J. T., Matthews, D. A., & Kraut, J. (1982) *J. Biol. Chem. 257*, 13663–13672.

Howell, E. E., Villafranca, J. E., Warren, M. S., Oatley, S. J., & Kraut, J. (1986) *Science (Washington, D.C.) 231*, 1123–1128.

Johnson, K. A. (1983) *J. Biol. Chem. 258*, 13825–13832.

Johnson, K. A. (1986) *Methods Enzymol. 134*, 677–705.

Kallen, R. G., & Jencks, W. P. (1966) *J. Biol. Chem. 241*, 5845–5850.

Lakowicz, J. R. (1983) *Principles of Fluorescence Spectroscopy*, Plenum, New York.

Mathews, C. K., & Huennekens, F. M. (1960) *J. Biol. Chem. 235*, 3304–3308.

Mathews, C. K., & Huennekens, F. M. (1963) *J. Biol. Chem. 238*, 3436–3442.

Matthews, D. A., Bolin, T. J., Burridge, J. M., Filman, D. J., Volz, K. W., Kaufman, B. T., Beddell, C. R., Champness, J. N., Stammers, D. K., & Kraut, J. (1985) *J. Biol. Chem. 260*, 381–391.

Mayer, R. J., Chen, J.-T., Taira, K., Fierke, C. A., & Benkovic, S. J. (1986) *Proc. Natl. Acad. Sci. U.S.A. 83*, 7718–7720.

Nixon, P. F., & Blakley, R. F. (1968) *J. Biol. Chem. 243*, 4722–4731.

P-L Biochemicals (1961) Circular OR-18, P-L Biochemicals, Milwaukee, WI.

Paulsen, H., & Wintermeyer, W. (1986) *Biochemistry 25*, 2749–2756.

Penner, M. H., & Frieden, C. (1985) *J. Biol. Chem. 260*, 5366–5369.

Smith, G. K., Benkovic, P. A., & Benkovic, S. J. (1981) *Biochemistry 20*, 4034–4036.

Srinivasan, R., & Fisher, H. F. (1985) *J. Am. Chem. Soc. 107*, 4301–4305.

Stone, S. R., & Morrison, J. F. (1982) *Biochemistry 21*, 3757–3765.

Stone, S. R., & Morrison, J. F. (1983) *Biochim. Biophys. Acta 745*, 247–258.

Stone, S. R., & Morrison, J. F. (1984) *Biochemistry 23*, 2753–2758.

Taira, K., Chen, J.-T., Fierke, C. A., & Benkovic, S. J. (1987a) *Bull. Chem. Soc. Jpn.* (in press).

Taira, K., Chen, J.-T., Mayer, R. J., & Benkovic, S. J. (1987b) *Bull. Chem. Soc. Jpn.* (in press).

Velick, S. F. (1958) *J. Biol. Chem. 233*, 1455–1467.

Villafranca, J. E., Howell, E. E., Voet, D. H., Strobel, M. S., Ogden, R. C., Abelson, J. N., & Kraut, J. (1983) *Science (Washington, D.C.) 222*, 782–788.

Viola, R. E., Cook, P. F., & Cleland, W. W. (1979) *Anal. Biochem. 96*, 334–340.

Williams, J. W., Morrison, J. F., & Duggleby, R. G. (1979) *Biochemistry 18*, 2567–2573.